京都大学防災研究所年報 第 53 号 B 平成 22 年 6 月
Annuals of Disas. Prev. Res. Inst., Kyoto Univ., No. 53 B, 2010

Two and Three Dimensional Slope Stability Analysis of Landslide Dam Failure due to Sliding

Ram Krishna REGMI*, Hajime NAKAGAWA, Kenji KAWAIKE, Yasuyuki BABA and Hao ZHANG

* Graduate School of Engineering, Kyoto University

Synopsis

Water flow in unsaturated porous media is water- air two-phase flow problem. To incorporate the effect of pore air flow in the soil seepage analysis a water-air two-phase flow model, based on the multi-phase flow theory is used. Slope stability analysis of land slide dam has been carried out using pore water pressure and moisture content calculated by only a conventional water-phase flow model as well as the water-air two-phase flow model so as to predict the failure of dam due to sudden sliding. Janbu's simplified method as well as extended Spencer method based on limiting equilibrium considerations is used in slope stability analysis. Overall simulation results obtained by considering two-phase seepage flow combined with extended Spencer method of slope stability analysis are comparatively in good agreement with the experimentally observed results.

Keywords: two-phase flow, variably saturated soil, landslide dam, slope stability

1. Introduction

Landslide dams (i.e., the natural blockage of river channels by hill slope-derived mass movements, Costa and Schuster, 1988) are natural phenomena with great relevance on geo-morphological conditions and on the safety of people. In areas placed upstream, respect to the river dammed section, waters blocked by the dam may provoke floods spreading for kilometers, causing damage to human activities and interrupting communication lines. Catastrophic outburst floods and/or debris flows can be triggered by a rapid dam failure with exceptional rates of sediment erosion and deposition along the downstream part of the valley.

Landslide dams commonly form in mountainous areas of high relief (Costa and Schuster, 1988), where there is sufficient input from both tectonic (earthquakes, hill slope gradients, relief) and climatic (precipitation, snowmelt) controls. About 90% of some 390 landslide dams examined worldwide were triggered by either rainstorms/snowmelts or earthquakes (Schuster, 1993), although other less common causes, such as volcanic (e.g., Umbal and Rodolfo, 1996; Melekestsev et al., 1999) or even anthropogenic activity (e.g., Asanza et al., 1992), have been documented.

Landslide dams fail by a variety of processes including overtopping, piping, overtopping by a landslide-generated wave, slope failure of upstream or downstream face, and the effects of human activity, usually an attempt to excavate a spillway over the debris dam. Many landslide dams fail shortly after their formation (Costa and Schuster, 1988). Figure 1 shows the dam longevity curve constructed considering sample of 73 documented

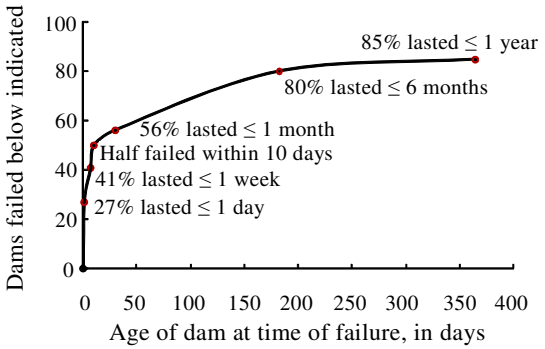

Fig. 1 Survival time before the failure of landslide dams, based on 73 cases from the literature and the authors' experience (Source: Costa and Schuster, 1988)

landslide dam failures; 27 percent of the landslide dams failed less than one day after formation, while 85 per cent within a year. Schuster (1993, 1995) argued that about 55% of some 187 investigated examples worldwide had failed within one week of their formation, whereas 89% failed after one year.

Landslide dam failure has been frequently studied as an earthen dam failure despite of their differences in geometry, dimensions and material properties. In depth knowledge of the failure mechanisms of the landslide dam and measured data are still being lacked. Numerical models from international literature allow to roughly computing the hydrograph resulting from the dam failure, (Fread 1991; Giuseppetti and Molinaro, 1989; Macchione and Sirangelo, 1988) however not giving any indications regarding the whole dam stability. Very few models are developed for landslide dam failure that can treat both the sediment and debris flow. Most of the existing models are applicable to overtopping failure of landslide dam. A numerical model has been developed (Awal et al., 2008) that can predict the time at which landslide dam may fail and also detect the failure mode either due to overtopping or due to sliding as well as the resulting out flow hydrograph.

Numerical and experimental studies were performed to investigate the mechanism of landslide dam failure by sliding (Awal et al., 2007, Awal, 2008). The pressure based Richards' equation descritized by finite difference technique was used in seepage flow model to determine moisture movement in the dam body. This model was then combined with transient slope stability model to get the dam failure time and the geometry of the failure surface.

Traditional methods of slope stability analysis assume that the soil is fully saturated. However, throughout much of the world, slopes exist in residual soil deposits. Such soils are often unsaturated, and the traditional saturated approach to assessing these slopes is inadequate. In looking at the behaviour of unsaturated soils, some authors (e.g. Dakshanamurthy et al, 1984) incorporate airflow within the soil, and it is clear that this aspect can be significant to the overall behaviour of the soil.

In this study conventional water-phase as well as water-air two-phase seepage flow numerical simulation models are developed individually for seepage calculation inside the body of landslide dam. Seepage flow model is then combined with transient slope stability model to predict the failure of dam due to sudden sliding. Simulation results are compared with the experimental measurements carried out by Awal (2008).

2. Numerical Modeling

Numerical models can be valuable tools in the prediction of seepage and the slope stability analysis. In the present analysis single-phase seepage flow model calculates the pore water pressure and moisture content inside the dam body where as the two-phase model calculates the pore water pressure, pore air pressure, and moisture content. Slope stability model uses the pore water pressure and moisture content obtained by the seepage flow model as in put data to calculate the critical slip surface and the corresponding factor of safety simultaneously.

2.1 Seepage flow Model

Seepage analysis may be required in volume change prediction, ground water contamination control, slope stability analysis, and the design of earth structures such as dykes or dams. To develop the seepage flow model, the governing equations are solved by line successive over relaxation (LSOR) scheme used by Freeze (1971, 1978) by an implicit iterative finite difference scheme.

(1) Single-phase flow model

Awal (2008) has used the following two and three dimensional pressure based Richards' equations to calculate the change in pore water pressure in variably saturated soil.

Two dimensional equation:

$$C\frac{\partial h}{\partial t} = \frac{\partial}{\partial x}\left(K_x\frac{\partial h}{\partial x}\right) + \frac{\partial}{\partial z}\left(K_z\left(\frac{\partial h}{\partial z}+1\right)\right) \quad (1)$$

Three dimensional equation:

$$C\frac{\partial h}{\partial t} = \frac{\partial}{\partial x}\left(K_x\frac{\partial h}{\partial x}\right) + \frac{\partial}{\partial y}\left(K_y\frac{\partial h}{\partial y}\right) + \frac{\partial}{\partial z}\left(K_z\left(\frac{\partial h}{\partial z}+1\right)\right) \quad (2)$$

where, h is the water pressure head; K_x, K_y and K_z are the hydraulic conductivity in x, y and z directions respectively; $C = \partial\theta/\partial h$ is the specific moisture capacity, θ is the soil volumetric water content; t is the time; x and y are the horizontal spatial coordinates; and z is the vertical spatial coordinate taken as positive upwards.

In order to solve the equations (1) and (2) following constitutive relationships proposed by Van Genuchten (1980) are used for establishing relationship of moisture content and water pressure head (θ-h), and unsaturated hydraulic conductivity and moisture content(K-θ):

$$S_e = [1 + (|\alpha h|)^{\eta}]^{-m} \quad (3)$$

$$S_e = \frac{\theta - \theta_r}{\theta_s - \theta_r} \quad (4)$$

$$K = K_s S_e^{0.5}[1 - (1 - S_e^{\frac{1}{m}})^m]^2 \quad (5)$$

where, S_e is the effective saturation; α and η are empirical parameters; θ_s and θ_r are saturated and residual moisture content respectively; K_s is the saturated hydraulic conductivity; and m=1-1/η.

(2) Two-phase flow model

Water flow in variably saturated soils is two-phase flow problem. The expedient approximation that air pressure is constant leads to the Richards' equation. To fully and accurately model variably saturated soils, both the air and water phases should be treated separately, with pressure and flow of both of these phases tracked within the model. In this study following two and three-dimensional equations are derived for the simultaneous flow of water and air based on the one-dimensional flow equations derived by Touma et al, (1986):

Two dimensional equations can be described as follows.

Water-phase equation is

$$C\left(\frac{\partial h_a}{\partial t} - \frac{\partial h_w}{\partial t}\right) = \frac{\partial}{\partial x}\left(K_{wx}\frac{\partial h_w}{\partial x}\right) + \frac{\partial}{\partial z}\left(K_{wz}\left(\frac{\partial h_w}{\partial z}+1\right)\right) \quad (6)$$

Air-phase equation is

$$\left((Ø-\theta)\frac{\rho_{0a}}{h_0} - \rho_a C\right)\frac{\partial h_a}{\partial t} + \rho_a C\frac{\partial h_w}{\partial t} = \frac{\partial}{\partial x}\left(\rho_a K_{ax}\frac{\partial h_a}{\partial x}\right) + \frac{\partial}{\partial z}\left(\rho_a K_{az}\left(\frac{\partial h_a}{\partial z}+\frac{\rho_a}{\rho_{0w}}\right)\right) \quad (7)$$

Three dimensional equations can be described as follows.

Water-phase equation is

$$C\left(\frac{\partial h_a}{\partial t} - \frac{\partial h_w}{\partial t}\right) = \frac{\partial}{\partial x}\left(K_{wx}\frac{\partial h_w}{\partial x}\right) + \frac{\partial}{\partial y}\left(K_{wy}\frac{\partial h_w}{\partial y}\right) + \frac{\partial}{\partial z}\left(K_{wz}\left(\frac{\partial h_w}{\partial z}+1\right)\right) \quad (8)$$

Air-phase equation is

$$\left((Ø-\theta)\frac{\rho_{0a}}{h_0} - \rho_a C\right)\frac{\partial h_a}{\partial t} + \rho_a C\frac{\partial h_w}{\partial t} = \frac{\partial}{\partial x}\left(\rho_a K_{ax}\frac{\partial h_a}{\partial x}\right) + \frac{\partial}{\partial y}\left(\rho_a K_{ay}\frac{\partial h_a}{\partial y}\right) + \frac{\partial}{\partial z}\left(\rho_a K_{az}\left(\frac{\partial h_a}{\partial z}+\frac{\rho_a}{\rho_{0w}}\right)\right) \quad (9)$$

where, h_w is the water pressure head; h_a is the air pressure head; h_0 is the atmospheric pressure expressed in terms of water column height; $C = \partial\theta / \partial h_c$ is the specific moisture capacity, $h_c = h_a - h_w$ is the ; ρ_a is density of air; ρ_{0a} is density of air at the atmospheric pressure; ρ_{0w} is density of water at the atmospheric pressure; K_{wx}, K_{wy} and K_{wz} are the hydraulic conductivity in x, y and z directions respectively; K_{ax}, K_{ay} and K_{az} are the air conductivity in x, y and z directions respectively; $C = \partial\theta / \partial h$ is the specific moisture capacity, Ø is the porosity of soil; θ is the soil volumetric water content; t is the time; x and y are the horizontal spatial coordinates; and z is the vertical spatial coordinate taken as positive upwards.

In order to solve the equations (6), (7), (8) and (9) following constitutive relationships proposed by Van Genuchten (1980) are used:

$$S_e = [1 + (\alpha_a h_c)^{\eta_a}]^{-m_a} \quad (10)$$

$$S_e = \frac{\theta - \theta_r}{\theta_s - \theta_r} \quad (11)$$

$$K_w = K_{ws} S_e^{0.5} \left[1 - \left(1 - S_e^{\frac{1}{m_a}}\right)^{m_a}\right]^2 \quad (12)$$

$$K_a = K_{as}(1 - S_e)^{0.5} \left[\left(1 - S_e^{\frac{1}{m_a}}\right)\right]^{2m_a} \quad (13)$$

where, S_e is the effective saturation; α_a and η_a are empirical parameters; $m_a = 1 - 1/\eta_a$; θ_s and θ_r are saturated and residual moisture content respectively; K_{ws} is the saturated hydraulic conductivity; K_{as} is the saturated air conductivity.

$$K_{as} = K_{ws} \frac{\mu_w}{\mu_a} \quad (14)$$

where, μ_w and μ_a are dynamic viscosity of water and air. $\mu_w = 1.002 * 10^{-3}$ NS/m^2 and $\mu_a = 1.83 * 10^{-5}$ NS/m^2 at 20°c.

2.2 Slope Stability Model

The stability of a slope depends on its geometry, soil properties and the forces to which it is subjected to internally and externally. The numerous methods currently available for slope stability analysis provide a procedure for assigning a factor of safety to a given slip surface, but do not consider the problem of identifying the critical conditions. Limit equilibrium method of slices is widely used for slope stability analysis due to its simplicity and applicability. In the method of slices, the soil mass above the slip surface is divided into a number of vertical slices and the equilibrium of each of these slices is considered. The actual number of the slices depends on the slope geometry and soil profile. The limiting equilibrium consideration usually involves two steps; one for the calculation of the factor of safety and the other for locating the most critical slip surface which yields the minimal factor of safety. Methods by Bishop, Janbu, Spencer and Morgenstern and Price are now well known.

In this study Janbu's simplified method as well as Spencer method has been incorporated into an effective minimization procedure based on dynamic programming by which the minimal factor of safety and the corresponding critical non circular slip surface are determined simultaneously. Janbu's simplified method only satisfies force equilibrium for the entire sliding mass and assumes resultant inter-slice forces horizontal where as Spencer/extended Spencer method satisfies both the force and moment equilibrium and assumes resultant inter-slice forces are at some angle to the horizontal. Fig. 2 shows the two dimensional general slip surface and forces acting on a typical slice and Fig. 3 shows the three dimensional general slip surface and forces acting on a typical column.

2-D and 3-D expressions of factor of safety F_s for Janbu's simplified method are as follows:

For 2-D Case;

$$F_s = \frac{1}{\sum_{i=1}^{n} W_i \tan\alpha_i} \times \sum_{i=1}^{n} \left\{ \frac{c l_i \cos\alpha_i + (W_i - u_i\, l_i \cos\alpha_i) \tan\emptyset}{\cos^2\alpha_i \left(1 + \frac{1}{F_s}\tan\alpha_i \tan\emptyset\right)} \right\} \quad (15)$$

where W_i is the weight of each slice including surface water, l_i is the length of the base of each slice, u_i is the average pore water pressure on the base of the slice, α_i is the inclination of the base to the horizontal, n is the total number of slices, and c and Ø are the Mohr-Coulomb strength parameters.

For 3-D Case;

$$F_s = \frac{\sum_{i=1}^{m}\sum_{j=1}^{n}\frac{\left[(c - u_{ij}\tan\emptyset)\Delta x\Delta y + (W_{ij} + P_{ij})\tan\emptyset\right]}{\left[\left(\frac{1}{J} + \frac{1}{F_s}\sin\alpha_{xzij}\tan\emptyset\right)\cos\alpha_{xzij}\right]}}{\sum_{i=1}^{m}\sum_{j=1}^{n}(W_{ij} + P_{ij})\tan\alpha_{xzij}} \quad (16)$$

where, $J = \left(1 + \tan^2\alpha_{xzij} + \tan^2\alpha_{yzij}\right)^{\frac{1}{2}}$, W_{ij} is the weight of column, P_{ij} is the vertical external force acting on the top of the column, Δx and Δy are discretized widths of the columns in x and y directions respectively, α_{xzij} and α_{yzij} are the inclination angles of the column base to the horizontal direction in the xz and yz planes respectively, m and n are the total number of columns in x and y directions respectively, and c and $\emptyset$ are the Mohr-Coulomb strength parameters.

The factor of safety expressions for Spencer method (Bardet, et al., 1989) and extended Spencer method (Jiang et al., 2004) in cases of 2-D and 3-D respectively are as follows:

For 2-D Case;

$$F_f = \frac{\sum_{i=1}^{n}\left\{\frac{cl_i + (W_i\cos\alpha_i - u_i\, l_i)\tan\emptyset}{m_\alpha}\right\}}{\sum_{i=1}^{n}\left\{\frac{W_i\sin\alpha_i}{m_\alpha}\right\}} \quad (17)$$

$$F_m = \frac{\sum_{i=1}^{n}\left\{\frac{cl_i + (W_i\cos\alpha_i - u_i\, l_i)\tan\emptyset}{m_\alpha}\right\} R_i\cos(\theta_i - \delta)}{\sum_{i=1}^{n}\left\{\frac{W_i\sin\alpha_i}{m_\alpha}\right\} R_i\cos(\theta_i - \delta)} \quad (18)$$

where, F_f = factor of safety with respect to force equilibrium, F_m = factor of safety with respect to moment equilibrium, $m_\alpha = \cos(\alpha_i - \delta)\left(1 + \frac{1}{F_f}\tan(\alpha_i - \delta)\tan\emptyset\right)$, δ= inclination of inter-slice forces to the horizontal, R_i = distance from the base centre of the slice to an arbitrary reference point, and θ_i = angle between the vertical direction and the R_i direction.

F_f and F_m can separately be computed from the equations (17) and (18) for several appropriately given values of δ. Then, two curves showing the relationships of $F_f - \delta$ and $F_m - \delta$ can be plotted so that the intersection of these two curves leads to a required value of factor of safety F_s, satisfying both force and moment equilibrium.

where, $m_\alpha = (1 + \tan\delta\tan\alpha_{xzij})/J + (\sin\alpha_{xzij} - \tan\delta\cos\alpha_{xzij})\tan\emptyset/F$ with $F = F_f$ for Eq. (19) and F_m for Eq. (20), δ = inclination of inter-slice forces to the x-axis, R_{ij} = distance from the axis of rotation to the base centre of a column in xz plane, and θ_{ij} = angle between the horizontal direction and the R_{ij} direction in the xz plane.

Factor of safety F_s, satisfying both force and moment equilibrium can be computed as mentioned in the case of 2-D.

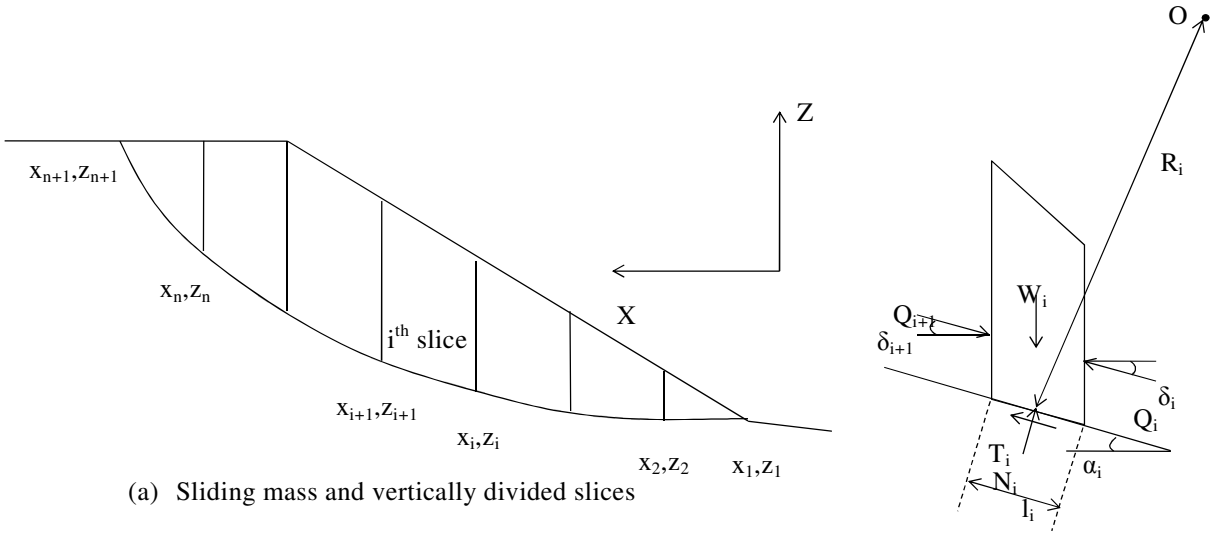

(a) Sliding mass and vertically divided slices

(b) Forces acting on the slice i

Fig. 2 Two dimensional general slip surface and forces acting on a typical slice

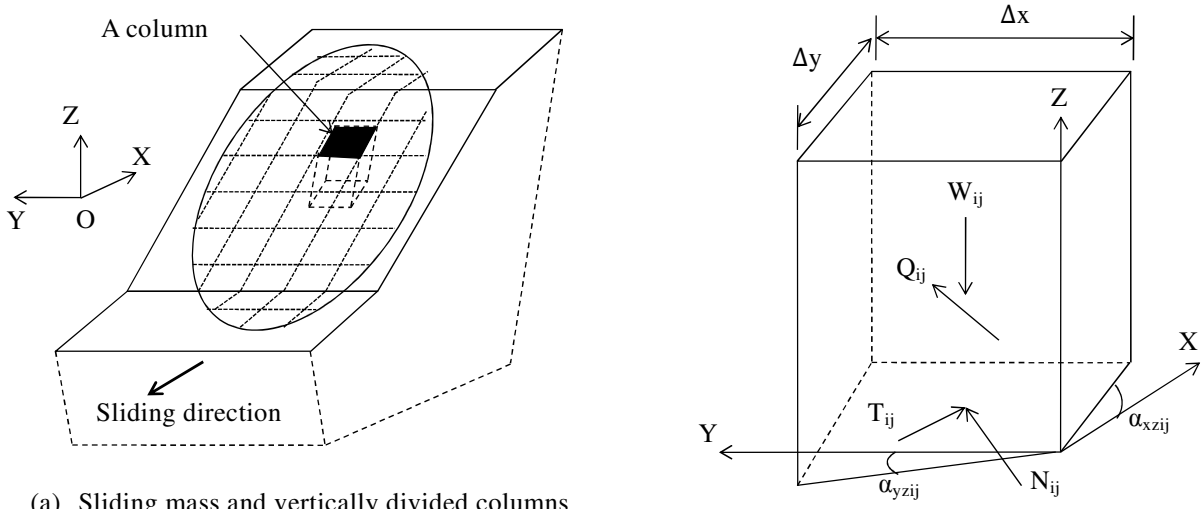

(a) Sliding mass and vertically divided columns

(b) Forces acting on a the column ij

Fig. 3 Three dimensional general slip surface and forces acting on a typical column

For 3-D Case;

$$F_f = \frac{\sum_{i=1}^{m}\sum_{j=1}^{n}\left[\begin{array}{l}\left(c - u_{ij}\tan\emptyset\right)\sec\alpha_{xzij}\,\Delta x\,\Delta y + \left(W_{ij}\right.\\ \left.+P_{ij}\right)\left\{\begin{array}{l}\left(\sec\alpha_{xzij} - \tan\delta\,\sin\alpha_{xzij}\right)\\ \tan\emptyset + F_f\tan\delta\dfrac{\tan^2\alpha_{xzij}}{J}\end{array}\right\}\end{array}\right]}{m_\alpha}}{\sum_{i=1}^{m}\sum_{j=1}^{n}\left(W_{ij}+P_{ij}\right)\tan\alpha_{xzij}} \quad (19)$$

$$F_m = \frac{\sum_{i=1}^{m}\sum_{j=1}^{n} R_{ij}\left[\begin{array}{c}\left(c - u_{ij}\tan\emptyset\right)\sec\alpha_{xzij}\,\Delta x\,\Delta y\\ \sin\left(\theta_{ij}+\delta\right)/\cos\delta + \left(W_{ij}+P_{ij}\right)\\ \cos\left(\theta_{ij}+\alpha_{xzij}\right)\\ \left\{\begin{array}{l}\tan\emptyset\,\tan\left(\theta_{ij}+\alpha_{xzij}\right)\\ +F_m\sec\alpha_{xzij}/J\end{array}\right\}\end{array}\right]/m_\alpha}{\sum_{i=1}^{m}\sum_{j=1}^{n}\left(W_{ij}+P_{ij}\right)R_{ij}\cos\theta_{ij}} \quad (20)$$

3. Experimental Test

Experimental results obtained by Awal (2008) are compared with the simulation results so as to evaluate the capability of the model. In his study (Awal, 2008), he considered constant water level and the steady discharge in the upstream reservoir in case of two-dimensional experiments and sready discharge in the upstream reservoir in case of three-dimensional experiments.

In case of two-dimensional experiments a rectangular flume of length 5m, width 20cm and depth 21cm was used. The slope of the flume was set at 17°. A rectangular flume of 5m long, 30cm wide and 50cm deep was used in case of three-dimensional experiments. The slope of the flume was set at 20°. The rectangular shape of the flume was modified to make cross slope of 20° so that the height of the dam is 30cm in one side and decreased uniformly towards other side to 19.08cm.

Triangular dam was prepared on the rigid bed of flume by placing mixed silica sand (Mix 1-7) on the flume. Water content reflectometers (WCRs) were used to measure the temporal variation of moisture content during seepage process. Red colored sediment strips were placed in the dam body at the flume wall face so as to measure the movement of the dam slope during sliding. The two-dimensional and three-dimensional landslide dams with the arrangement of WCRs are schematically shown in Figure 4 and Figure 5 respectively.

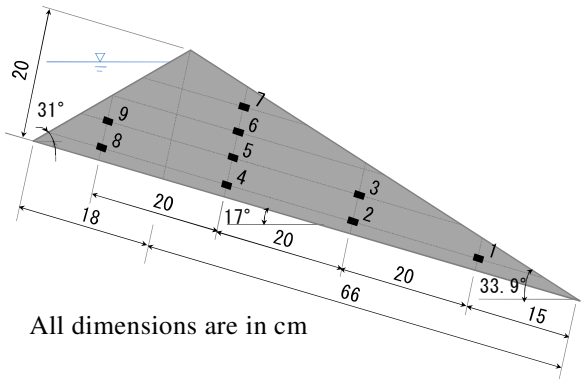

All dimensions are in cm

Fig. 4 Two dimensional dam body shape and size with the arrangements of WCRs (1-9)

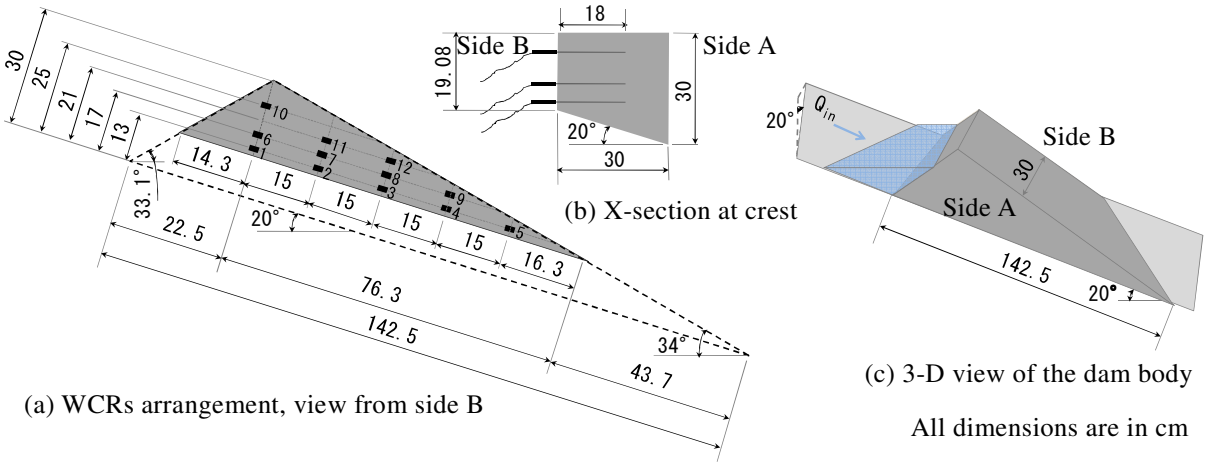

(a) WCRs arrangement, view from side B

(b) X-section at crest

(c) 3-D view of the dam body

All dimensions are in cm

Fig. 5 Three dimensional dam body shape and size with the arrangements of WCRs (1-12)

4. Results and Discussions

In two dimensional analysis numerical simulation has been carried out with space step of 2 mm and time step of 0.004 second in seepage flow model and longitudinal space step (parallel to dam base) of 6 cm and time step of 1 second in slope stability model. In three dimensional analysis numerical simulation has been carried out with space step of 1 cm and time step of 0.01 second in seepage flow model and longitudinal space step of 5 cm, lateral space step of 3 cm and time step of 1 second in slope stability model.

In case of 2-D experiment with constant water level in the upstream reservoir, water level at 16 mm below the crest level of the dam was maintained in 25 seconds and the sudden sliding of the dam was observed at 255 seconds. The simulated failure time using Janbu's simplified method of slope stability analysis is 222 and 231 seconds in conventional and water-air two-phase seepage flow considerations respectively where as the failure time using Spencer method of slope stability analysis is 248 and 257 seconds in conventional and water-air two-phase seepage flow considerations respectively. Figure 6 shows the simulated and experimental moisture content profiles at WCR-4, WCR-6 and WCR-8 and Figure 8 shows the simulated and experimental slip surfaces.

In case of 2-D experiment with steady discharge in the upstream reservoir, 39.8 cm^3/sec discharge was maintained and the sudden sliding of the dam was observed at 350 seconds. The simulated failure time using Janbu's simplified method of slope stability analysis is 305 and 304 seconds in conventional and water-air two-phase seepage flow considerations respectively where as the failure time using Spencer method of slope stability analysis is 323 and 322 seconds in conventional and water-air two-phase seepage flow considerations respectively. Figure 7 shows the simulated and experimental moisture content profile at WCR-4, WCR-6 and WCR-8 and Figure 9 shows the simulated and experimental slip surfaces.

In case of 3-D steady discharge in the upstream reservoir, 29.8 cm^3/sec discharge was supplied and the sudden sliding of the dam was observed at 930 seconds. The simulated failure time using Janbu's simplified method of slope stability analysis is 768 and 777 seconds in conventional and water-airtwo-phase seepage flow considerations respectively where as the failure time using extended Spencer method of slope stability analysis is 793 and 802 seconds in conventional and water-air two-phase seepage flow considerations respectively. Figure 10 shows the simulated and experimental moisture content profile at WCR-2, WCR-4 and WCR-8 and Figure 11 shows the simulated and experimental slip surfaces.

Simulated and experimental moisture profiles are satisfactorily in agreement although results comparison shows some simulated results have faster moisture movement than that of experimental one and some have slower movement. Also the simulated failure shapes are matching satisfactorily with experimental failure shapes of all considered cases. From the view point of safety before and

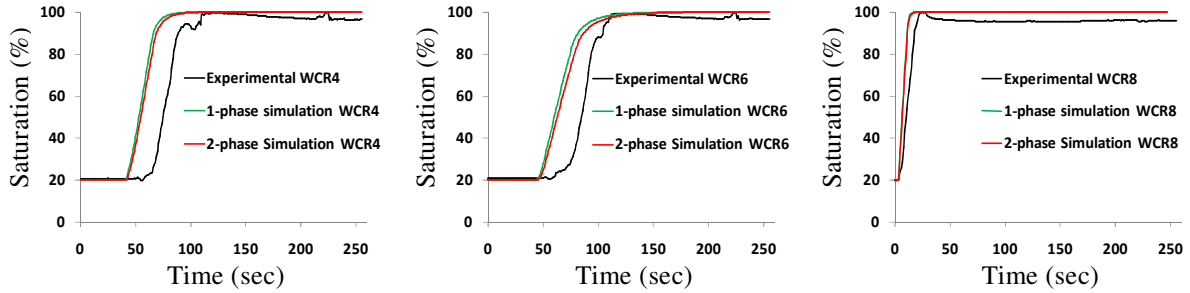

Fig. 6 Simulated and experimental moisture content profiles for constant head in upstream reservoir (2D case)

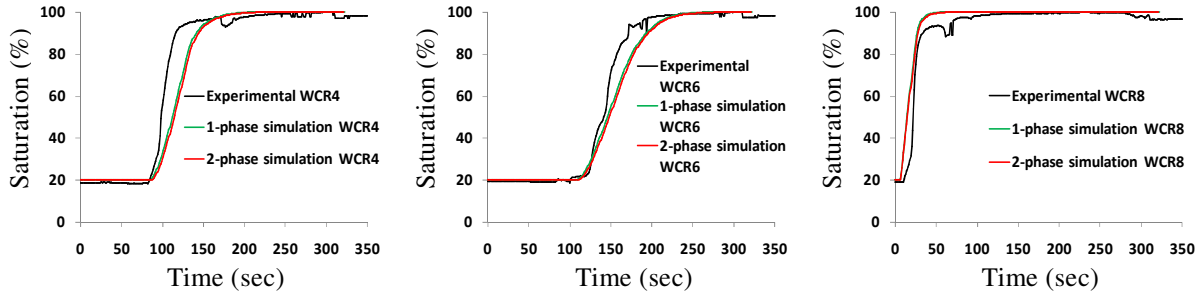

Fig. 7 Simulated and experimental moisture content profiles for steady discharge in upstream reservoir (2D case)

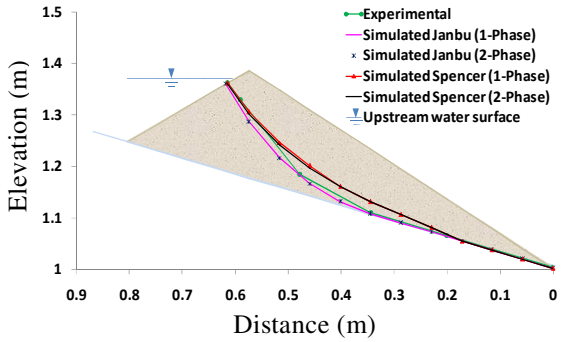

Fig. 8 Simulated and experimental critical slip surfaces for constant head in upstream reservoir (2D case)

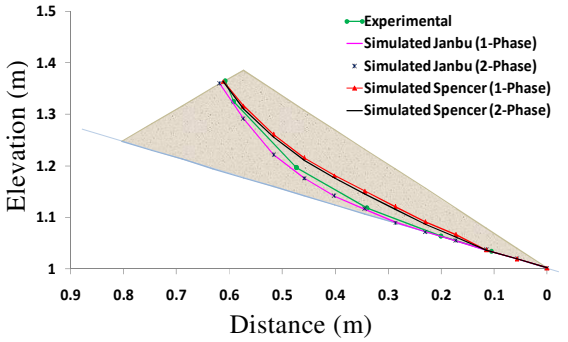

Fig. 9 Simulated and experimental critical slip surfaces for steady discharge in upstream reservoir (2D case)

after the failure of dam the most important is the prediction of dam body failure time rather than the failure shape. In all the cases, failure time computed by Spencer/extended Spencer method is quite closer to the experimentally observed failure time than the failure time computed by Janbu's simplified method.

Saturated hydraulic conductivity Ks is a key parameter for guiding the moisture profile and failure time of dam body which depends on the sand mix and its compaction. It is difficult to ensure uniformity of sand mix and its compaction during Ks test and formation of experimental dam body. So it is better to have record the temporal variation of upstream reservoir head during experiment so that Ks value can be played during simulation to get more accurate simulated reservoir head that may lead simulated moisture movement and dam failure time quite closer to experimental one.

Actually air become trapped in the voids by the infiltrating water from the upstream reservoir, initially causing compression of the air phase, leading to a reduction in the rate of water infiltration. The air pressure will increase until it reaches a sufficient value for the air to escape by bubbling. This phenomenon has not been

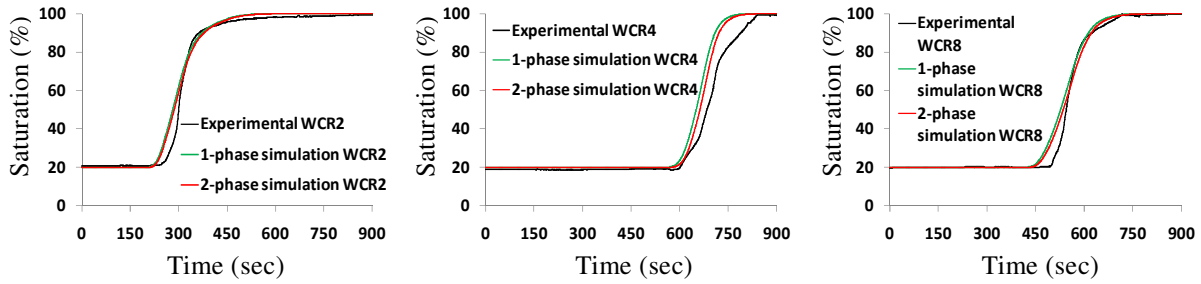

Fig. 10 Simulated and experimental moisture content profiles for steady discharge in upstream reservoir (3D case)

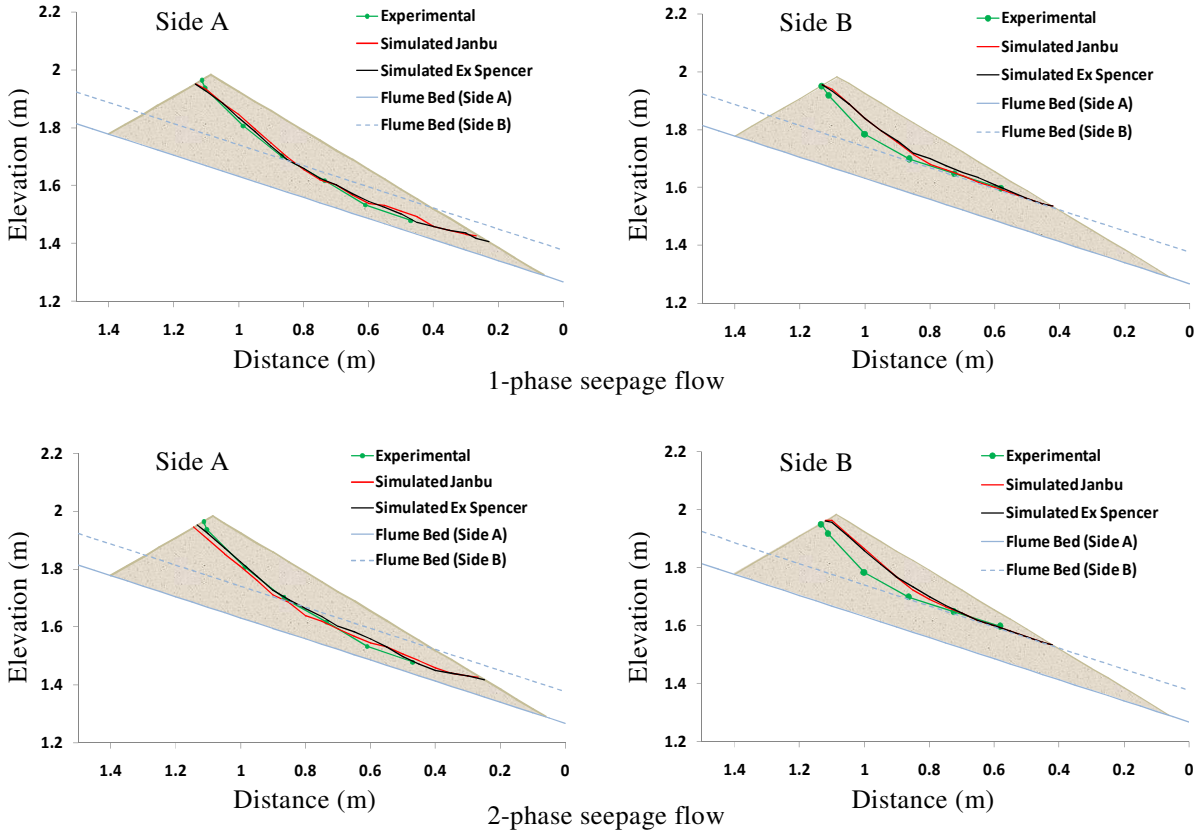

Fig. 11 Simulated and experimental critical slip surfaces for steady discharge in upstream reservoir (3D case)

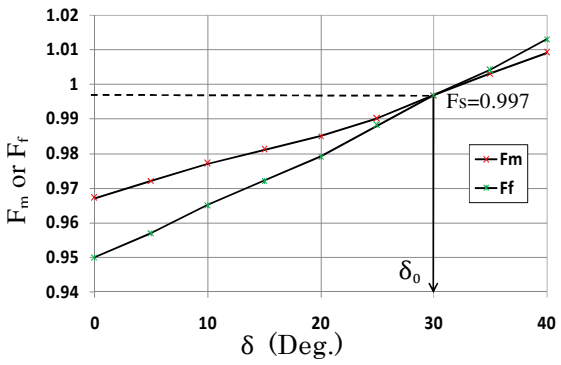

Fig. 12 Typical relationships of F_m-δ and F_f-δ

considered in conventional seepage flow model but the water-air two-phase flow model has been considered it. Hence simulated moisture profiles obtained by the two-phase seepage flow model are slightly delayed than that of conventional seepage flow model. Ultimately, failure time of the dam body has also found to be delayed while considering two-phase seepage flow in Janbu's simplified method as well as Spencer/extended Spencer method in the cases of 2-D constant head and 3-D steady discharge. Since there was flow path for the air phase in the dam body laterally

toward downstream and vertically up beyond the reservoir water ponding reach, the difference of predicted failure times considering only one-phase and two-phase seepage flow is not so much large.

It is already mentioned in section 2.2 that Janbu's simplified method only satisfies force equilibrium for the entire sliding mass and assumes resultant interslice forces horizontal where as Spencer/extended Spencer method satisfies both the force and moment equilibrium and assumes resultant interslice forces are at some angle δ_0 to the horizontal. Hence the factor of safety calculated by the Janbu's simplified method is less than that of Spencer/extended Spencer method in a given condition, resulting failure time of the dam body earlier in case of Janbu's simplified method. Choosing δ values from 0^0~40^0 at 5^0 intervals, required δ_0 value was evaluated for calculating factor of safety F_s using Spencer/extended Spencer method as mentioned in section 2.2. The F_m- δ and F_f- δ relationships obtained during simulation of 3D case, considering two-phase flow seepage analysis, are typically shown in Fig. 12. Required δ_0 along with the corresponding Fs is also presented in the same figure.

5. Conclusions

The comparison of experimental and simulated results shows that the results obtained by water-air two-phase seepage flow model and extended Spencer method of slope stability analysis is more closer to the experimental results than that of conventional seepage flow model and Janbu's simplified method of slope stability analysis even though simulated failure time is much earlier than that of experimental in steady discharge cases of 2-D and 3-D. More experimental studies as well as sensitivity analysis are necessary to get experimental and simulated results quite close. The performance of the model can further be improved by incorporating more rigorous method of slope stability analysis that also considers the influence of pore air pressure in the soil slope stability. It is recommended to carry out the experimental measurement of air pressure at different points inside the dam body so that the result that may be obtained by the simulation can be verified.

References

Asanza, G.P., Yepes, H., Schuster, R.L., Ribadeneira, S. (1992): Landslide blockage of the Pisque River, Northen Ecuador, In Bell DH (ed) Landslides, Glissements de terrain, Proceedings of the sixth international symposium, Christchurch, 1229–1234.

Awal, R., Nakagawa, H., Baba, Y. and Sharma, R. H. (2007): Numerical and experimental study on landslide dam failure by sliding, Annual Journal of Hydraulic Engineering, JSCE, Vol.51, pp.7-12.

Awal, R., Nakagawa, H., Kawaike, K., Baba, Y. and Zhang, H. (2008): An integrated approach to predict outflow hydrograph due to landslide dam failure by overtopping and sliding, Annual Journal of Hydraulic Engineering, JSCE, Vol. 52, pp.151-156.

Awal, R. (2008): Study on Landslide Dam Failure Due to Sliding and Overtopping, Doctoral Thesis, Kyoto University.

Bardet, J.P. and Kapuskar, M.M. (1989): A simplex analysis of slope stability, Computers and Geotechnics, 8, 329-348.

Costa, J.E. and Schuster R.L. (1988): The formation and failure of natural dam, Geological Society of America Bulletin 100, 1054–1068.

Costa, J.E. and Schuster, R.L. (1991): Documented historical landslide dams from around the world, US Geological Survey Open File Report, 91–239.

Dakshanamurthy, V., Fredlund, D.G. and Rahardjo, H (1984): Coupled three dimensional consolidation theory of unsaturated porous media, Proceedings of the fifth international conference on expansive soils, Adelaide, South Australia.

Fread D. (1991): The NWS dambrk model: theoretical background/user documentation, National Weather Service, NOAA: Silver Spring, Maryland.

Freeze, R.A. (1971a): Three dimensional transient, saturated unsaturated flow in a groundwater basin, Water Resour. Res., Vol.7, pp.347-366.

Freeze, R.A. (1971b): Influence of the unsaturated flow domain on seepage through earth dams, Water Resour. Res., Vol.7, pp.929-941.

Freeze, R. A. (1978): Mathematical models of hillslope hydrology, in Kirkby, M. J., ed., Hillslope Hydrology, John Wiley, pp. 177-225.

Giuseppetti, G. and Molinaro, P. (1989): A mathematical model of the erosion of an embankment dam by overtopping, Proceedings of International Symposium on analytical evaluation of dam related safety problems, Copenhagen.

Jiang, J.-C. and Yamagami, T.(2004): Three-dimensional slope stability analysis using an extended Spencer method, Soils and Foundations, Japanese Geotechnical Society, Vol. 44, No. 4, 127-135.

Macchione, F. and Sirangelo, B. (1988): Study of earth dam erosion due to overtopping, Proceedings of technical conference of hydrology of disasters, WMO, Ginevra.

Schuster, R.L. (1993): Landslide dams—a worldwide phenomenon, In Proceedings annual symposium of the Japanese Landslide Society, Kansai Branch, 27 April, Osaka, 1–23.

Schuster, R.L. (1995): Landslide dams—a worldwide phenomenon, J Jpn Landslide Soc 31(4), 38–49.

Touma, J. and Vauclin, M.(1986): Experimental and numerical analysis of two-phase infiltration in a partially saturated soil, Transport in Porous Media, 1, 27–55.

Umbal, J.V., Rodolfo, K.S. (1996): The 1991 lahars of southwestern Mount Pinatubo, Philipines, and evolution of the lahar-dammed Mapanuepe Lake, In Newhall CG, Punongbayan RS (eds) Fire and mud eruptions and lahars of Mount Pinatubo, University of Washington Press, Philippines sattle, pp. 951–970.

Van Genuchten, M.T. (1980): A closed-form equation for predicting the hydraulic conductivity of unsaturated soils, Soil Sci. Soc. Am. J., Vol.44, pp892–898.

地すべりによる天然ダム決壊の二次元および三次元斜面安定解析

Ram Krishna REGMI*, 中川一・川池健司・馬場康之・張浩

*京都大学大学院工学研究科

要　旨

不飽和多孔質媒体内の流れは，水と空気の２相流れの問題となる。本研究では間隙内空気の流れの効果を考慮するために，多相流理論に基づき水と空気の２相流モデルの導入を行った。これまで天然ダムの斜面の安定解析では，突然の決壊を予測するために，間隙水圧と含水率を解く従来の水相流モデル，水と空気の２相流モデルによって解析されており，そのモデル内はJanbuの簡易的な方法だけでなく，平衡状態に基づいた拡張Spencer法などが用いられている。本研究では，拡張Spencer法を用いて２相流れを解析しており，実験結果とも比較的良く一致した結果が得られている。

キーワード: ２相流，飽和土，天然ダム，斜面安定